Electronic and optical properties of SnTe and GeTe

Electronic and optical properties of SnTe and GeTe

C M I Okoye

Department of Physics and Astronomy, University of Nigeria, Nsukka, Nigeria

E-mail: okoyecmi@yahoo.com

Abstract
The structural properties, electronic energy band structure and some optical
properties of the IV–VI compounds SnTe and GeTe are calculated using
the full-potential linearized augmented plane wave method within the local
density approximation and the generalized gradient approximation schemes.
The calculations were also performed incorporating the effects of spin–orbit
interactions. The calculated structural properties, energy band structures
and optical spectra are in reasonable agreement with available experimental
data. The response of the bandgaps to temperature and the presence of some
prominent features in the energy bands as well as the dielectric functions are
discussed.

1. Introduction

The IV–VI semiconducting compounds $A^{IV}B^{VI}$ (A^{IV} = Ge, Sn, Pb; B^{VI} = S, Se, Te) are
important in several practical applications as infra-red lasers in fibre optics, as thermoelectric
materials in solar energy panels and in window coatings [1–4]. In addition, they also possess
some unusual and possibly unique properties such as high dielectric constant and high carrier
mobility as well as a narrow fundamental gap of several tenths of an electron volt at the L point.
As a result of their narrow fundamental gap, the IV–VI semiconductors are suitable as infrared
detectors and light emitting devices. All these have over the years helped in motivating the study
of their optical and electronic properties both theoretically [5–12] and experimentally [13–16].

The band structures and optical properties of some other IV–VI semiconductors such as
PbS, PbSe and PbTe [5, 17, 18] have been theoretically obtained by a variety of methods
but there is very little such information (to the best of our knowledge) about SnTe and GeTe
using any of the modern first-principles electronic structure techniques. One of the aims of
the present study is to provide improved energy bands based on a first-principles technique
which hopefully will reduce the uncertainty present in current theoretical interpretations of
experimental spectra. In our present paper, the optical properties and electronic structure of
the IV–VI compounds, SnTe and GeTe will be carried out using the full-potential linearized

augmented plane wave (FP-LAPW) method within the framework of the density functional approach.

It is well known that above its transition temperature, SnTe crystallizes in the rocksalt (NaCl) structure. GeTe, on the other hand, is face centred rhombic; however, the distortion from fcc is small, and we have assumed, as is usually the case, the rocksalt structure also. The experimental lattice constants are 6.327 Å [19] and 5.996 Å [20] for SnTe and GeTe respectively. Furthermore, they have a direct minimum energy bandgap of 0.23 [21] and 0.20 eV [22] at the L point in the Brillouin zone.

The band structures of SnTe and GeTe have been calculated using many different techniques which include the empirical pseudopotential method [10, 11], the augmented plane wave method [8], the orthogonalized plane wave method [11] and the *ab initio* pseudopoential method [6]. All these methods gave results that show several common features in these compounds but they differ in detail in comparison with experimental data. In this study, we shall employ a first principles technique: the FP-LAPW method within the density functional theory (DFT) which is known to give very satisfactory results when compared with experimental data in order to account for the finer features of the band structures of these compounds. The methodology of the FP-LAPW method as embodied in the WIEN97 code [23] will be used in the study of the electronic, structural and optical properties of SnTe and GeTe.

It is known that within the density functional approach, the effects of exchange and correlation are treated using the standard local density approximation (LDA) or the generalized gradient approximation (GGA). Studies have shown that using the LDA leads to some discrepancies (e.g. an underestimation of the equilibrium lattice constant and an overestimation of the bulk modulus) between theoretical and experimental results [24–26]. Some of these discrepancies are on average somewhat improved upon by the introduction of the GGA [27, 28] which introduces corrections to the LDA exchange–correlation functional through the gradient of the charge density. It is one of the objectives of this work to investigate the suitability or otherwise of these (LDA and GGA) approximation schemes in the study of the electronic properties of SnTe and GeTe. To this end, among the GGAs available, the particular GGA of interest is the Perdew–Burke–Ernzerhof (PBE) [29] type GGA, which is constructed by preserving and extending the correct formal properties of LDA. The PBE-GGA reduces the LDA overbinding and greatly improves the atomization energies; it gives realistic binding energy curves for rare-gas dimers where other GGAs fail as well as improving lattice constants and magnetic properties of many metals [30]. However, sometimes, GGA reproduces experimental phenomena; in other cases the GGA overestimates the LDA results [31].

We are aware that spin–orbit (SO) coupling is a relativistic effect which scales with the atomic number of the atom. Thus for compounds containing fairly heavy elements, such as Sn and Te, one expects the effect of SO coupling to be non-negligible. However, even in crystals such as Ge, the relativistic (mass–velocity and Darwin corrections) are quite substantial [32]. Thus, the SO coupling effects need to be included in the study, for proper elucidation of the electronic structure of the compounds (SnTe and GeTe). As a result, in this work, we incorporate the SO effects while employing both the LDA and the PBE-GGA respectively to account for the exchange and correlation effects. This will enable us to perform a comparative analysis of the results obtained for these compounds using the two exchange and correlation approximation techniques within the same computational framework provided by the WIEN97 code.

The optical properties of IV–VI semiconductor SnTe have been previously obtained by means of near-normal incidence reflectivity measurements [13, 16]. However, recently, spectroscopic ellipsometry (SE) measurements were reported for SnTe [15]. The SE technique is better than other methods because both the real and imaginary parts of the dielectric functions are obtained directly on a wavelength-by-wavelength basis without having to resort to multiple

non-simultaneous measurements or Kramers–Kronig analysis. Furthermore, it is well known that the dielectric function $\epsilon(\omega)$ of a semiconductor is closely related to its electronic energy band structure. As such, using the ellipsometry data, their studies complement each other in providing detailed information about their band structures and optical properties.

The organization of the paper is as follows: we present the computational method in section 2. The results are presented and discussed in section 3. In section 4, we draw conclusions from the study.

2. Computational procedure

In the present study, the FP-LAPW method within the DFT is used. We use the WIEN97 implementation of the FP-LAPW method, the details of which are discussed in [23]. In this method, no shape approximation on either the potential or the electronic charge density is made. The exchange and correlation energy is calculated within the LDA using the Perdew–Wang [33] reparametrization of the Ceperley–Alder data and within the GGA scheme using the PBE-GGA. The self-consistent calculations are based on the following parameters: SnTe crystallizes in the sodium chloride (rocksalt) structure with two atoms per unit cell. We have assumed for this study that GeTe also crystallizes in the same rocksalt structure. The space group is $Fm3m$ which has 48 symmetry operations and includes inversion symmetry. The muffin-tin sphere radii of Sn, Ge and Te have been chosen to be 2.3, 2.0 and 2.3 au respectively. Within these spheres, the charge density and potentials are expanded in terms of crystal harmonics, and a plane wave expansion has been used in the interstitial region. The Brillouin zone integration has been performed with 47 k points in the irreducible part of the Brillouin zone. A satisfactory convergence was achieved by considering a number of FP-LAPW basis functions up to $R_{MT}K_{max} = 9$, where K_{max} is the maximum value of the plane wavevector and R_{MT} is the muffin-tin atomic radius. Both the muffin-tin radius and the number of k points are varied to ensure convergence. In order to keep the same degree of convergence throughout the calculations, we kept all the values of the sphere radii and K_{max} constant. All electrons are treated self-consistently. The energy as a function of atomic volume, and the energy band structure, were calculated with and without SO coupling using both LDA and PBE-GGA forms of exchange–correlation potential.

For the calculation of the optical properties, a dense mesh of uniformly distributed k points is required. Hence, the Brillouin zone integration was performed using the tetrahedron method with 165 k points in the irreducible part of the Brillouin zone without broadening. The dielectric function ($\epsilon(\omega) = \epsilon_1(\omega) + i\epsilon_2(\omega)$) is known to describe the optical response of the medium at all photon energies $E = \hbar\omega$. In this study, the imaginary part of the dielectric function ($\mathrm{Im}[\epsilon(\omega)]) = \epsilon_2(\omega)$ is given as in [34] by

$$\mathrm{Im}[\epsilon(\omega)] = \epsilon_2(\omega) = \left(\frac{4\pi^2 e^2}{m^2\omega^2}\right) \sum_{i,j} \int \langle i|M|j\rangle^2 f_i(1-f_j)\delta(E_f - E_i - \omega)\,\mathrm{d}^3k \tag{1}$$

where M is the dipole matrix, i and j are the initial and final states respectively, f_i is the Fermi distribution function for the ith state and E_i is the energy of an electron in the ith state. The real part ($\epsilon_1(\omega)$) of the dielectric function can be extracted from the imaginary part using the Kramers–Kronig relation in the form

$$\mathrm{Re}[\epsilon(\omega)] = \epsilon_1(\omega) = 1 + \frac{2}{\pi} P \int_0^k \frac{\omega' \epsilon_2(\omega')\,\mathrm{d}\omega'}{(\omega'^2 - \omega^2)} \tag{2}$$

where P implies the principal value of the integral.

Table 1. Calculated equilibrium lattice constant (a_{eq}), bulk modulus, B_0, and pressure derivative of bulk modulus, B'.

	Without SO		With SO		
Compound	LDA	GGA	LDA	GGA	Expt
SnTe (a_{eq}) (Å)	6.231	6.404	6.235	6.407	6.327
(B_0) (GPa)	50.750	40.066	49.982	39.649	42[a]
(B')	4.470	4.256	4.332	4.678	
GeTe (a_{eq}) (Å)	5.858	6.011	5.862	5.995	5.996
(B_0) (GPa)	60.015	48.930	59.412	48.060	
(B')	4.404	4.106	4.668	4.073	

[a] See [36].

For a given photon energy (ω), the real part of the absorption coefficient (α) is expressed in the form

$$\alpha = \frac{2\pi\omega}{c}\sqrt{\frac{-\mathrm{Re}(\epsilon) + |\epsilon|}{2}}. \tag{3}$$

3. Results and discussion

3.1. Total-energy calculations

The ground state bulk properties of SnTe and GeTe were obtained using the calculations of total energy as a function of volume within the FP-LAPW method using the LDA and PBE-GGA exchange and correlation schemes. These calculations were then repeated with SO coupling effects included. The total energy curves were obtained by calculating the total energy at a minimum of five different volumes around the equilibrium volume and fitting the calculated values to the Murnaghan equation of state [35]. From these total-energy versus atomic volume curves, the zero-pressure equilibrium lattice constant (a_{eq}), bulk modulus (B_0) and pressure derivative of bulk modulus (B') were obtained. The values obtained are displayed in table 1 together with the available experimental data [36].

It is observed that for SnTe, the values of the equilibrium lattice constant obtained using either the LDA or PBE-GGA exchange and correlation schemes fall within the same degree of accuracy ($\pm 1.5\%$) of the experimental value. On the other hand, for GeTe the PBE-GGA results are in better agreement with experimental data than the LDA calculations. It is further observed that the inclusion of SO coupling effects leads to slight improvements in the values obtained for a_{eq} irrespective of the type of exchange and correlation effect. In addition, the inclusion of SO coupling leads to the lowering of the total energy by about 0.005 and 0.006 Ryd for GeTe and SnTe respectively. The bulk modulus calculated using PBE-GGA for SnTe agrees fairly well with experimental results. When compared with other theoretical calculations, we find that, in general, our study of the structural properties give results that are closer to experiment.

3.2. Energy band structure

The band structures of SnTe and GeTe along the principal symmetry directions have been calculated. The experimental values of the lattice constant for the respective compounds were used for calculations. Figures 1 and 2 show the relativistic (with SO) band structure of SnTe and GeTe calculated using the PBE-GGA scheme for the exchange and correlation potential. The positions of the symmetry points are indicated by vertical lines. In figures 3 and 4, we
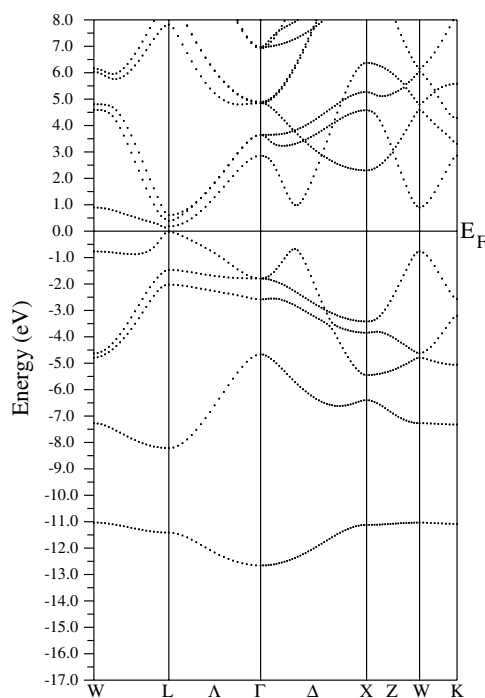
Figure 1. Electronic energy band structure of SnTe calculated using PBE-GGA including SO coupling.

display the band structure of both compounds calculated using PBE-GGA without including SO coupling. The bandgaps obtained from calculations with and without SO interaction using both LDA and PBE-GGA exchange and correlation schemes are displayed in table 2 together with the experimentally determined values. It is seen that the energy gaps obtained using the PBE-GGA and LDA schemes are comparable. Table 2 shows that for SnTe without SO coupling, the bandgaps obtained using both exchange–correlation schemes understimate the experimental data. This bandgap underestimation is not unusual in density functional calculations since the one-particle eigenvalues of the Kohn–Sham equations do not describe the excited states and hence, in general, do not compare well with experimental excitation energies. To correct this problem, the excited states (band structures) are calculated using the quasiparticle method [37–42] in which a non-local energy-dependent self-energy operator (Σ) replaces the exchange–correlation potential. Our result for GeTe without SO coupling which indicates that the bandgaps are overestimated is in contast to the expected LDA underestimation. It may well be that the quasiparticle self-energy operator is apparently well approximated by the effective one-electron potential of the ground state in this case. However, with the inclusion of SO coupling, close agreement is obtained when compared with experimental values for both compounds.

Our calculations also show that the valence band maximum (VBM) and conduction band minimum (CBM) are both at the L point of the Brillouin zone for both compounds. As such, they possess direct bandgaps.

The VBM results from a hybridization of 4s Ge and 5p Te bands. In the non-SO calculation, the next lower band to the VBM merges with the VBM on going from the L point along the Λ direction to the Γ point and along the Δ direction to the X point and to the W point. The inclusion of the SO coupling effects leads to some modifications of the bands, the most
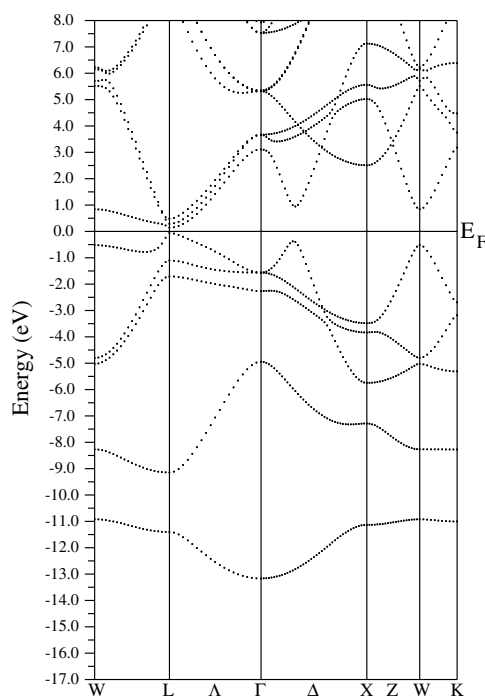
Figure 2. Electronic energy band structure of GeTe calculated using PBE-GGA including SO coupling.

Table 2. Theoretically calculated bandgaps using LDA and PBE-GGA with and without SO interaction at the experimental lattice constant.

	LDA (eV)	GGA (eV)	Expt (eV)
SnTe	0.074	0.061	0.20[a]
SnTe (with SO)	0.225	0.212	
GeTe	0.399	0.340	0.20[b]
GeTe (with SO)	0.244	0.201	

[a] See [21].
[b] See [22].

prominent of which is the presence of a gap between the second and third highest valence bands at the L point and through the Λ direction to the Γ point and subsequently to the W point. This is in contrast to the non-SO calculation in which these bands following the VBM are degenerate. This modifying effect on the bands due to the inclusion of SO coupling leads to improvement in the values of the bandgaps obtained for the compounds. It is seen from the figure that the VBM is split at both the L point and the Γ points for SnTe and GeTe respectively. Also at the X point, the effect of SO coupling splits the valence band for both SnTe and GeTe. The magnitude of SO splitting is in satisfactory agreement with available experimental results of [15] for SnTe. On the whole, our results reproduce the essential features of the band structures of SnTe and GeTe, prominent among which is the arrangement of band symmetries at the L point in which the valence and conduction bands have L_6^+ and L_6^- symmetries and vice versa for SnTe and GeTe in the double group notation. Furthermore, our results are in satisfactory agreement with results obtained in previous calculations [9–11].
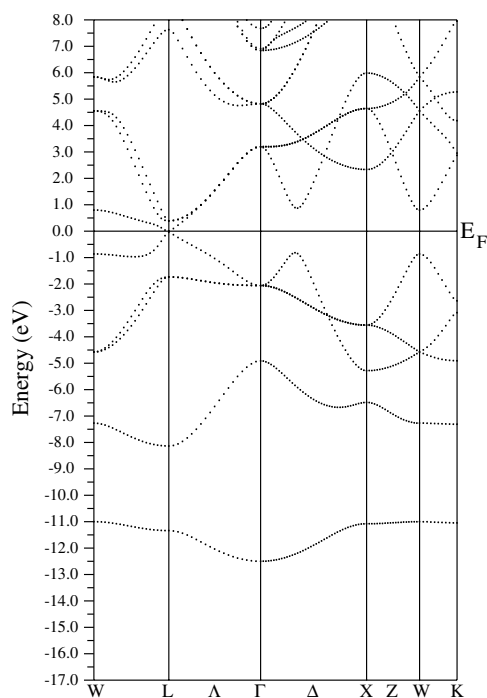
Figure 3. Electronic energy band structure of SnTe calculated using PBE-GGA without SO coupling.

Table 3. Calculated energy gap (E_g) for SnTe and GeTe at different lattice constants (a) within LDA and GGA schemes.

		SnTe			GeTe		
a (Å)		6.231	6.327	6.404	5.858	5.996	6.011
	LDA	0.207	0.074	0.022	0.153	0.399	0.424
E_g (eV)	GGA	0.200	0.061	0.043	0.083	0.340	0.367

The effect of pressure on the energy gap of the semiconductors has also been studied by calculating the energy gaps at different lattice constants using the two exchange and correlation schemes (LDA and PBE-GGA). This is shown in table 3.

It is observed by studying table 3 that the band gap in SnTe decreases with increase in the lattice constant. This could be interpreted to imply that it has negative temperature coefficient in agreement with experimental measurements [21, 43]. This behaviour is opposite to the trend found in GeTe. This dissimilar response of the bandgap to temperature change suggests that the principal band edges in GeTe are probably more like those of other IV–VI compounds such as PbTe where such a trend is found than SnTe. The response of the energy gap to change in lattice constant in GeTe is therefore contrary to expectation. However, it may be interpreted to arise as a result of our assumption of cubic rather than rhombic structure for GeTe at room temperature.
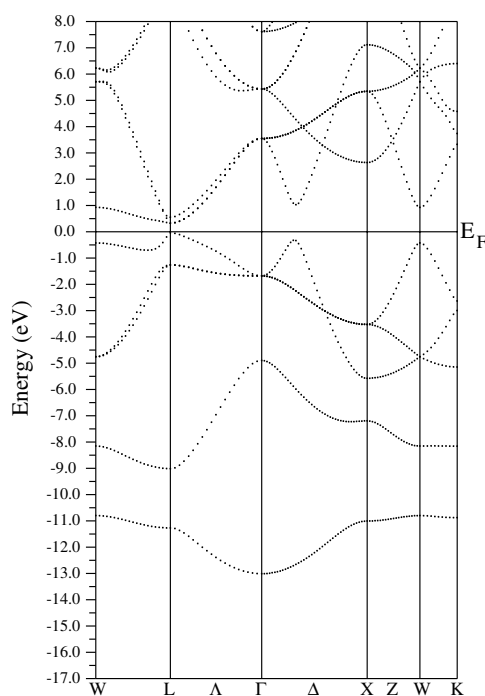
Figure 4. Electronic energy band structure of GeTe calculated using PBE-GGA without SO coupling.

3.3. Optical properties

The real (ϵ_1) and imaginary (ϵ_2) parts of the frequency dependent dielectric function ($\epsilon(\omega)$) for SnTe and GeTe have been calculated for photon energies up to 6 eV using equations (1) and (2) respectively within the framework of the LDA scheme for exchange and correlation along the lines prescribed in the WIEN97 optical package by Ambrosch-Draxl *et al* [23]. The results of calculations of optical properties performed using LDA without the SO effect are displayed in figures 5–8 for SnTe and GeTe. It is seen that in the dispersive part of the dielectric function, ϵ_1, shown in figures 5 and 6, the main features are fairly broad peaks around 1.0 eV for both compounds followed by a steep decrease between about 1.2 and 1.7 eV. After this, ϵ_1 becomes negative, a minimum and then slowly increases toward zero at higher energies. A significant difference between the $\epsilon_1(\omega)$ spectra in the two compounds is the presence of bumps in SnTe around 2.2 eV. This is in fair agreement with the experimental prediction of 2.45 eV. This feature is not present in the calculated GeTe spectra. The structures are more pronounced in the calculated spectra since these are not broadened. As seen in figures 5 and 6, ϵ_1 is zero at about 1.6 and 1.5 eV for SnTe and GeTe, respectively.

The absorptive part of the dielectric function, ϵ_2, is shown in figures 7 and 8 for SnTe and GeTe respectively. The calculated spectrum for SnTe has more structure than the experimental spectrum. It is seen that ϵ_2 is somewhat similar in the two compounds. Furthermore, for GeTe, the main peak is much narrower. The spectrum shown in figure 7 rises sharply above 0.5 eV with the highest peak at about 1.6 eV. The origin of this structure as suggested by Lin *et al* [10] comes from band transitions occurring along the Σ symmetry line around (0.42, 0.42, 0) while the decrease above the peak is attributed to a strong M_2 critical point from transitions along Δ.
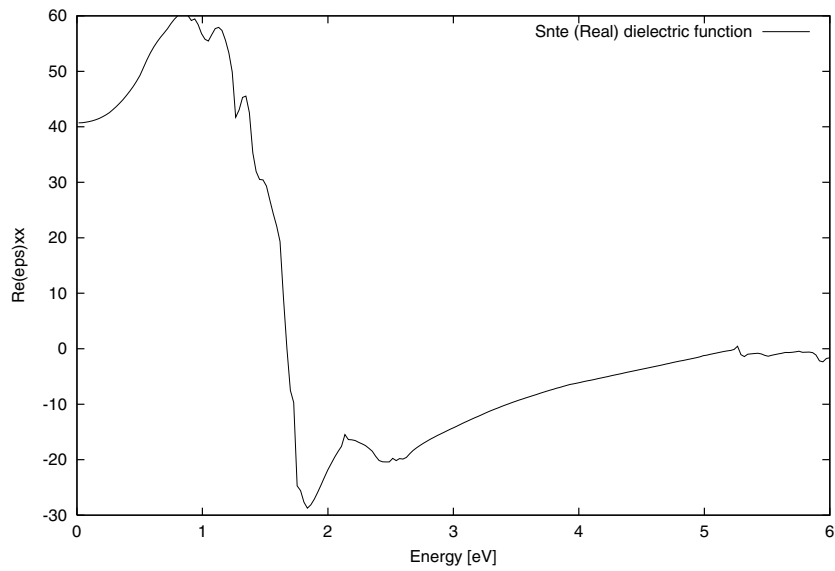
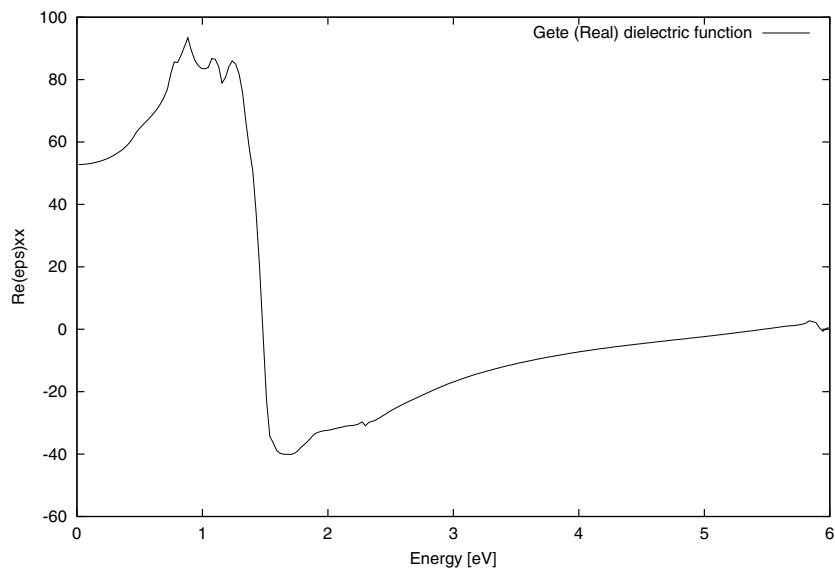**Figure 5.** Calculated real part of the dielectric function for GeTe.

Figure 6. Calculated real part of the dielectric function for GeTe.

The maximum amplitude of the calculated spectrum for SnTe is significantly higher than in the experimental spectrum. This is probably so because the calculated spectrum is unbroadened. We have also in figures 9 and 10 presented the absorption coefficient for the compounds GeTe and SnTe calculated using equation (3). The features observed in the experimental result for SnTe are fairly well reproduced in our calculations. It is generally observed that our calculations are in reasonable agreement with available theoretical results [10].
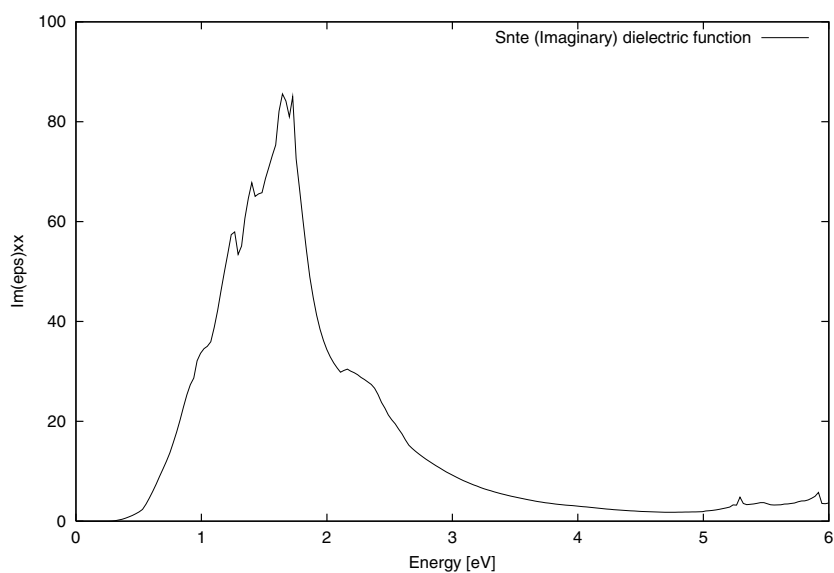
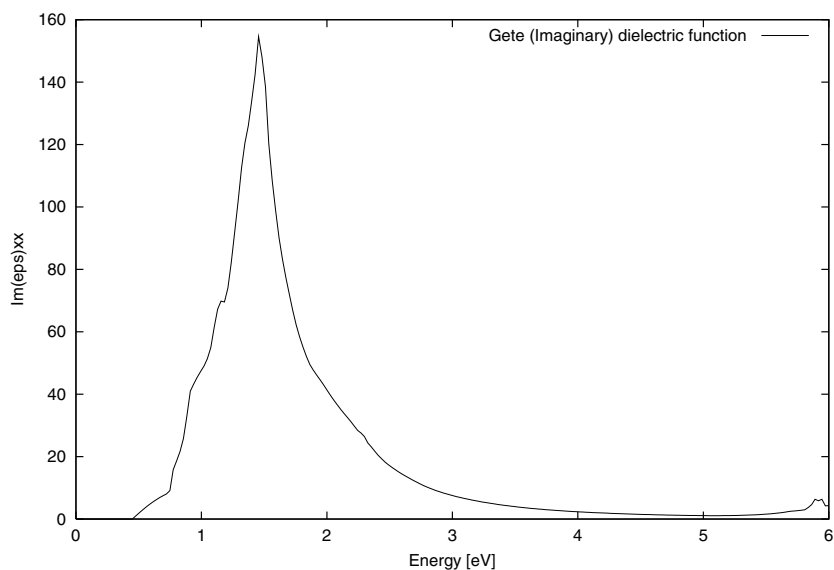**Figure 7.** Calculated imaginary part of the dielectric function for SnTe.

Figure 8. Calculated imaginary part of the dielectric function for GeTe.

4. Conclusions

We have presented in this study the structural, electronic and some optical properties of the binary semiconductor compounds SnTe and GeTe using the FP-LAPW method and employing the local density as well as the PBE GGAs to the exchange and correlation potentials. These calculations have been performed with and without SO coupling effects. We note that the inclusion of SO coupling effects generally improved the agreement between the parameters
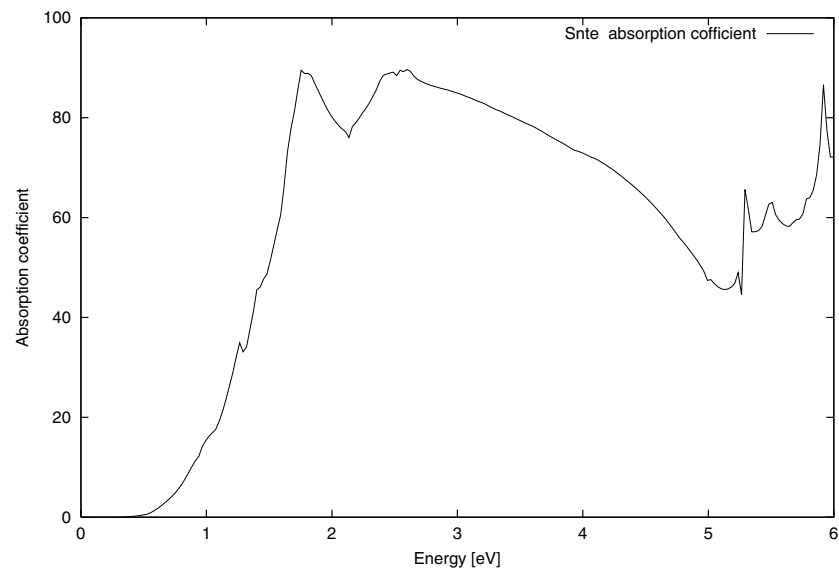
Figure 9. Numerically calculated spectral dependence of the absorption coefficient for SnTe.
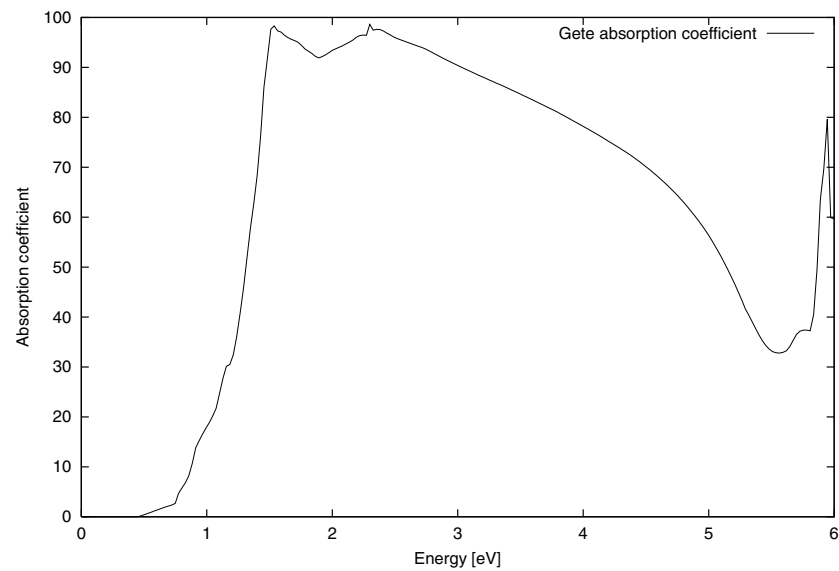

Figure 10. Numerically calculated spectral dependence of the absorption coefficient for GeTe.

studied (bandgap, lattice constant, bulk modulus) and the experimental data. Our results also show that the energy band structures are very well reproduced by our calculations. The optical properties such as the dielectric functions of rocksalt SnTe and GeTe are well described by our study. On the whole, this study shows that the structural, electronic and optical properties of SnTe and GeTe are fairly well accounted for using the FP-LAPW method.

Acknowledgments

References

[1] See, for example,
    Agrawal G P and Dutta N K 1993 *Semiconductor Lasers* (New York: Van Nostrand-Reinhold) p 547
[2] Hicks L D, Harman T C, Sun X and Dresselhaus M S 1996 *Phys. Rev.* R10 493
[3] Chatterjee S and Pal U 1993 *Opt. Eng.* **32** 2923
    Chaudhuri T K 1992 *Int. J. Energy Res.* **16** 481
    Mohamed M T 1990 *Solar Energy Mater.* **20** 2
[4] Nair P K, Ocampo M, Fernandez A and Nair M T S 1990 *Solar Energy Mater.* **20** 235
    Nair P K, Fernandez A and Nair M T S 1989 *Proc. SPIE Int. Soc. Opt. Eng.* **1149** 88
[5] Delin Anna, Ravindran P, Erickson P and Olle Wills J M 1998 *Int. J. Quantum Chem.* **69** 349
[6] Rabe K M and Joannopoulos J D 1985 *Phys. Rev.* B **32** 2302
[7] Cohen M L, Tung Y and Allen P B 1968 *J. Physique Coll.* **29** (Suppl.) C4 4–163
[8] Rabii S 1969 *Phys. Rev.* **182** 821
    Rabii S 1968 *Bull. Am. Phys. Soc.* **13** 413
[9] Tung Y W and Cohen M L 1969 *Phys. Rev.* **180** 823
[10] Lin P J, Saslow W and Cohen M L 1967 *Solid State Commun.* **5** 893
[11] Herman F, Kortum R L, Ortenburger I B and Van Dyke J P 1968 *J. Physique Coll.* **29** (Suppl.) C4 62
[12] Cohen M L and Bertgstresser T K 1966 *Phys. Rev.* **141** 789
[13] Korn D M and Braunstein R 1972 *Phys. Rev.* B **5** 4837
[14] Richard Burke J Jr and Reidl H R 1969 *Phys. Rev.* **184** 830
[15] Suziki N and Adachi S 1995 *Japan. J. Appl. Phys.* **34** 5977
[16] Cardona M and Greenaway D L 1964 *Phys. Rev.* A **133** 1685
[17] Albanesi A E, Okoye C M I, Rodriguez C O, Peltzer y Blanca E L and Petukhov A G 2000 *Phys. Rev.* B **61** 16 589
[18] Wei Su-Wei and Zunger A 1997 *Phys. Rev.* B **55** 13 605
[19] Bis R F and Dixon J R 1969 *J. Appl. Phys.* **40** 1919
[20] Tung Y W and Cohen M L 1969 *Phys. Rev.* **180** 823
[21] Esaki L and Stiles P J 1966 *Phys. Rev. Lett.* **16** 1108
    Esaki L 1966 *J. Phys. Soc. Japan* **21** 589
    Tsu R, Howard W E and Esaki L 1968 *Phys. Rev.* **172** 779
[22] Chang L L, Stiles P J and Esaki L 1966 *IBM J. Res. Dev.* **10** 484
[23] Blaha P, Schwarz K and Luitz L 1999 *WIEN97, a Full Potential Linearized Augmented Plane Wave Package for Calculating Crystal Properties* Technical University of Vienna
    This is an improved and updated Unix version of the original copyrighted WIEN code, which was published by
    Blaha P, Schwarz K, Sorantin P and Trickey S B 1990 *Comput. Phys. Commun.* **59** 399
[24] Paxton A T, Methfessel M and Polatoglou H M 1990 *Phys. Rev.* B **41** 8127
[25] Rubio A, Corkill J L, Cohen M L, Shirley E L and Louie S E 1993 *Phys. Rev.* B **48** 11 810
    Zhu X and Louie S E 1991 *Phys. Rev.* B **43** 14 142
[26] Vogel D, Kruger P and Pollmann J 1997 *Phys. Rev.* B **55** 12 836
[27] Bango P, Jepson O and Grunnarsson O 1989 *Phys. Rev.* B **40** 1997
[28] Korling M and Haglund J 1992 *J. Phys. Rev.* B **45** 13 293
[29] Perdew J P, Burke K and Ernzerhof M 1996 *Phys. Rev. Lett.* **77** 3865
    Perdew J P, Burke K and Ernzerhof M 1997 *Phys. Rev. Lett.* **78** 1396 (erratum)
[30] Perdew J P, Kurth S, Zupan A and Blaha P 1999 *Phys. Rev.* B **82** 2544
[31] Lee In-Ho and Martin R M 1997 *Phys. Rev.* B **56** 7197 and references therein
[32] Johnson L E, Conklin J B Jr and Pratt G W Jr 1963 *Phys. Rev. Lett.* **11** 538
    Herman F, Kuglin C D, Cuff K F and Kortum R L 1963 *Phys. Rev. Lett.* **11** 541
[33] Perdew J P and Wang Y 1992 *Phys. Rev.* B **45** 13 244
[34] Ambrosch-Draxl C and Abt R 1998 *The Calculation of Optical Properties within WIEN97 (ICTP Lecture Notes)* unpublished

[35] Murnaghan F D 1944 *Proc. Natl Acad. Sci. USA* **30** 244
[36] Sneddon T, Gupta S C and Saunders G A 1976 *Solid State Commun.* **20** 69
     Hoston B and Strakna R E 1964 *Bull. Am. Phys. Soc.* **9** 646
[37] Hedin L 1965 *Phys. Rev.* **139** A796
     Hedin L and Lundqvist 1969 *Solid State Physics* vol 23, ed H Ehrenreich, F Seitz and D Turnbull (New York: Academic) p 1
[38] Hybersten M S and Louie S G 1985 *Phys. Rev. Lett.* **55** 1418
     Hybersten M S and Louie S G 1986 *Phys. Rev.* B **34** 5390
[39] Godby R W, Schluter M and Sham L J 1986 *Phys. Rev. Lett.* **56** 2415
     Godby R W, Schluter M and Sham L J 1988 *Phys. Rev.* **37** 10 159
[40] Gygi F and Baldereschi A 1989 *Phys. Rev. Lett.* **2160**
[41] Zhu X and Louie S G 1991 *Phys. Rev.* B **43** 14 142
[42] Fleszar A and Hanke W 2000 *Phys. Rev.* B **62** 2466
[43] Dimmock J O, Melngailis I and Strauss A J 1966 *Phys. Rev. Lett.* **16** 1193